ACS APPLIED MATERIALS & INTERFACES

Research Article

Cite This: ACS Appl. Mater. Interfaces 2019, 11, 13105−13113

www.acsami.org

Wearable Fiber-Based Organic Electrochemical Transistors as a Platform for Highly Sensitive Dopamine Monitoring

Xing Qing,[†,‡,§] Yuedan Wang,*[,†,‡] Yang Zhang,[†,‡] Xincheng Ding,[†,‡] Weibing Zhong,[∥] Dong Wang,*[,‡,∥] Wenwen Wang,[†,‡] Qiongzhen Liu,[†,‡] Ke Liu,[†,‡] Mufang Li,[†,‡] and Zhentan Lu[†,‡]

[†]College of Materials Science and Engineering, Wuhan Textile University, Wuhan 430200, China

[‡]Hubei Key Laboratory of Advanced Textile Materials & Application, Wuhan 430200, China

[§]Institute for Frontier Materials, Deakin University, Waurn Ponds, Geelong, Victoria 3216, Australia

[∥]College of Chemistry, Chemical Engineering and Biotechnology, Donghua University, Shanghai 201620, China

Supporting Information

ABSTRACT: Fiber-based organic electrochemical transistors (FECTs) provide a new platform for the realization of an ultrafast and ultrasensitive biosensor, especially for the wearable dopamine (DA)-monitoring device. Here, we presented a fully filament-integrated fabric, it exhibited remarkable mechanical compatibility with the human body, and the minimum sensing unit was an organic electrochemical transistor (OECT) based on PVA-*co*-PE nanofibers (NFs) and polypyrrole (PPy) nanofiber network. The introduction of NFs notably increased the specific surface area and hydrophilicity of the PA6 filament, resulting in the formation of a large area of intertwined PPy nanofiber network. The electrical performance of PPy nanofiber network-modified fibers improved considerably. For the common FECTs, the typical on/off ratio was up to two orders of magnitude, and the temporal recovery time between on and off states was shortened to 0.34 s. Meanwhile, the device exhibited continuous cycling stability. In addition, the performances of FECT-based dopamine sensors depending on different gate electrodes have also been investigated. The PPy/NFs/PA6 filament-based dopamine sensor was more superior to the gold and platinum (Pt) wires, and the sensor presented long-term sensitivity with a detection region from 1 nM to 1 μM, rapid response time to a set of DA concentrations, remarkable selectivity in the presence of sodium chloride, uric acid, ascorbic acid and glucose, and superior reproducibility. Moreover, it could also be woven into the fabric product. The novel and wearable FECT device shows the potential to become the state-of-the-art DA-monitoring platform.

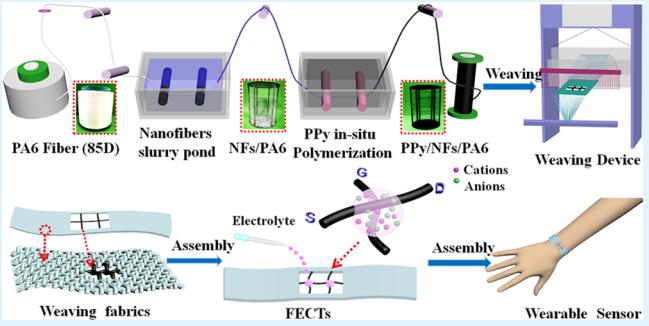

KEYWORDS: *Fiber-based organic electrochemical transistor, PVA-co-PE nanofibers, Polypyrrole nanofiber network, PA6 filament, Dopamine sensor*

1. INTRODUCTION

Dopamine (DA) is recognized as a critical neurotransmitter appearing in the forebrain and basal ganglia of a creature.[1] DA has received extensive attention when it is found to be implicated in the functions of renal, reward, hormonal, and cardiovascular systems and even the central nervous system.[2,3] The most notorious two diseases related to the dysfunctional metabolism of the dopaminergic neuron process are Parkinson's syndrome and Alzheimer's disease. The former is caused by the deficiency of dopamine-producing neurons, and the latter gives rise to dementia in the advanced stages.[4,5] Statistically, the population of people suffering from dementia worldwide reached up to 35.6 million in 2010. Furthermore, this number will double by 2030 and more than triple by 2050.[6] Apart from Parkinson's syndrome and Alzheimer's disease, the imbalance of dopamine levels also plays a vital role in schizophrenia disease, depressive disorder, somnipathy, and addictive behaviors, such as shopaholism and drug abuse.[7,8] The disastrous cost due to the abnormal metabolism of DA changed millions of households by increasing the economic burden on families and countries, eventually taking an urgent problem into account. However, the basal concentrations of DA in the extracellular fluid are merely micromoles (μM) in urine, nanomoles (nM) in plasma, and picomolar (pM) in pheochromocytoma and paraganglioma cells; such a low concentration dramatically increases the difficulty in clinical detection.[4] Consequently, it is of critical significance to quantitatively analyze DA levels in the extracellular fluid or biological system in routine diagnosis with excellent sensitivity, ultraselectivity, and fast response. To date, there are various typical analytical methods of DA concentrations in the reported research studies such as chemiluminescence,[9]

Received: January 3, 2019
Accepted: March 21, 2019
Published: March 21, 2019

DOI: 10.1021/acsami.9b00115
ACS Appl. Mater. Interfaces 2019, 11, 13105−13113

Scheme 1. Schematic Diagram of Wearable Dopamine Sensors Based on FECTs[a]

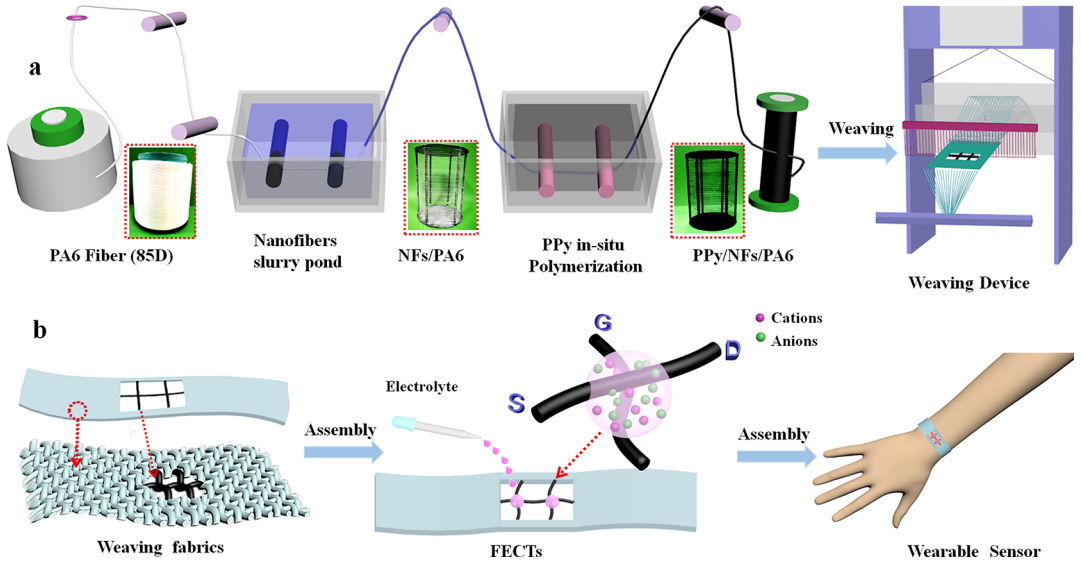

[a](a) Preparation process and weaving of coated fibers. (b) Assembly of the woven FECTs and wearable DA sensors.

capillary electrophoresis,[10] ultraviolet−visible and mass spectroscopy,[11] high-performance liquid chromatography,[12] and dominant electrochemistry detection.[13,14] However, most of them suffer from several drawbacks and cannot satisfy the requirements nowadays. Organic thin-film transistors (OTFTs) have been intensively investigated for the application of dopamine detection due to low cost, easy fabrication, and unprecedented portability.[15,16] Particularly, the organic electrochemical transistors (OECTs), an outstanding representative of OTFTs, have emerged and demonstrated to be the state-of-the-art platform for the point-of-care testing of glucose,[17] protein biomarkers,[18] dopamine,[19] lactate,[20] ions,[21,22] saliva,[23] DNA,[24] etc. Compared to OTFTs, the working voltage of OECTs is particularly low (~1 V), which can effectively avoid hydrolysis and adequately convert biochemical signals into an electronic one. From the viewpoint of all notable properties, OECTs have demonstrated the advantages to be applied in DA sensing applications. Tang et al. designed a highly sensitive OECT-based DA sensor by comparing different gate electrodes, including graphite, Au and Pt electrodes, etc.; the lowest detection limit to dopamine could reach about 5 nM.[3] However, the sensor has no selectivity to DA. Gualandi et al. fabricated a poly(3,4-ethylene dioxythiophene) (PEDOT:PSS)-based OECT sensor for selective detection of dopamine (DA) in the presence of interfering compounds, but the detection limit was 6 μM.[25] Yan et al. described the Nafion and graphene flake-modified gate electrode to increase the selectivity and sensitivity; the lowest detection concentration of the dopamine sensor is 5 nM,[15] while the Pt electrode is expensive and not suitable for practical applications. Hence, for the future wearable OECT-based dopamine sensors, the demands of a fabrication method with high sensitivity, fast response rate, low detection limit, and cost effectiveness as well as high flexibility should all be taken into consideration. In our early study,[26] the FECT-based glucose sensor exhibited higher sensitivity and selectivity compared to the planar configuration. This phenomenon can be attributed to the three-dimensional structures of fibers with a larger surface-to-volume ratio. This enlarged electroactive area of FECTs leads to a higher electrical signal, and then it is amplified by the transistor. Consequently, the FECTs can be more suitable for implementing complex and area-scalable e-textiles because of their excellent flexibility, ultrasensitivity, and feasibility of miniaturization.[27] In this paper, we designed all fiber-based organic electrochemical transistors, where the current amplification ratio and response rate notably outperformed traditional OECTs. In addition, the FECTs can be woven by a traditional loom as DA sensors. The PA6 filament was simply integrated with NFs and a PPy nanofiber network, respectively. However, the ultrafast response time, long-term stability, and superior reproducibility of the FECTs were significantly improved, owing to the mutual interlaced NF composite layer. Furthermore, the three-dimensional PPy nanofiber network was induced by the NFs to provide an effective platform for the high-performance FECT-based DA sensor. Performances of different Au, Pt, and fiber gate electrodes have been investigated. Compared to metal gate electrode-based FECT sensors, the fiber gate electrode had the largest initial channel current, superior sensibility even when the DA concentration was decreased to 1 nM, and outstanding selectivity under the presence of four interferents. All these merits suggest that the PPy/NFs/PA6-based FECT system can potentially be applied to detect DA.

2. EXPERIMENTAL SECTION

2.1. Materials. Poly(vinyl alcohol) (PVA), phosphoric acid, iron(III) nitrate nonahydrate, 5-sulfosalicylic acid dihydrate, sodium anthraquinone-2-sulfonate, sodium chloride, pyrrole, dopamine hydrochloride, ascorbic acid (AA), uric acid (UA), and glucose were purchased from Aladdin Reagent Database Inc. Phosphate-buffered saline (PBS) solution (pH 7) was supplied from Sigma-Aldrich Co. PA6 (85 D) was obtained from U.S. Pacific Nonwovens Industry Limited.

2.2. Preparation of PPy/PVA-*co*-PE/PA6 Filament. In this experiment, the raw 85 D (where D is denier) PA6 filament was first immobilized on a simple plastic ring to avoid the monofilament loosening. Subsequently, the immobilized filament was ultrasonicated in acetone, alcohol, and enough DI water successively before drying completely in the fume hood. Then, the processed PA6 filament was adequately immersed in 2 wt % NF suspension; the preparation method of NFs was published by our group previously.[28,29] After

DOI: 10.1021/acsami.9b00115
ACS Appl. Mater. Interfaces 2019, 11, 13105−13113

shaking for 2 h under room temperature, the filament was totally wrapped by the white NFs, but the final NFs/PA6 (85 D) composite was not obtained until the unbonded NFs on the surface was strongly blown away with a dryer. Next, PPy was synthesized on the surface of the NFs/PA6 filament surface by the in situ polymerization method.[26,30] First, the NFs/PA6 fiber was fully immersed in a yellowish-brown solution, which was made up of a pyrrole monomer (12 g/L), deionized (DI) water, and sodium anthraquinone-2-sulfonate (10 g/L), and then the mixed solution with the sample ring was sealed and vibrated gently for 10 min to ensure that all the pyrrole monomers uniformly adhered on the NFs/PA6 surface; this process played a key role in the consecutive growth of PPy. Second, the mixed solution with the sample ring was put in the refrigerator. Simultaneously, another bottle of the same volume solution with an oxidizing agent was put in the refrigerator. The main ingredients of the oxidizing agent solution were 5-sulfosalicylic acid dihydrate, iron(III) nitrate nonahydrate (the mole ratio was 1:1), and DI water. Third, after 10−15 min, these two solutions were taken out; the mixed solution with the sample ring was stirred under a motor stirrer, while the oxidizing agent solution was added into the yellowish-brown solution dropwise for about 10−20 min. All of the operations and polymerization were implemented in an ice bath for 4 h under 800 rpm of continuous stirring. The obtained PPy/NFs/PA6 (85 D) was successively washed with running water, ethyl alcohol, and DI water and then dried completely in the fume hood before use. The reference sample of PPy/PA6 was obtained according to the same polymerization process.[31,32]

2.3. Fabrication of FECTs and Sensors Based on FECTs. Scheme 1 shows the schematic diagram of a novel mass production technique to manufacture the FECT-oriented dopamine sensor. As shown in Scheme 1a, the PA6 filament was first adequately sized in the NF slurry pond and then sufficiently surface conductive-treated with PPy, the end product FECTs were fabricated by PPy/NFs/PA6 (85 D) conducting fibers. Obviously, the FECT device unit was directly integrated into a plain weave fabric product by the loom machine. By designing the fabric texture, a one-step preparation of FECT with different circuit configuration could be easily accomplished and much more effective compared to other large-scale preparation methods. The structure parameters of FECTs are particularly illustrated in Figure S1 (Supporting Information). These two conducting fibers were a cross-junction configuration and were separated by a certain volume of transparent gel electrolyte, which is for highly sensitive dopamine sensing. The assembly process of the FECT-oriented DA sensor is shown in Scheme 1b. A certain volume of transparent gel electrolyte was added to the center of the completely separated source−drain and gate fibers to integrate the FECTs. The woven and ultraflexible FECTs are expected to have a potential application in highly sensitive dopamine sensing.

2.4. Characterization and Electrochemical Measurements of FECTs and FECT-Based Dopamine Sensor. The main electrochemical tests and characteristic curves were investigated by a Keithley 4200SCS semiconductor parameter analyzer. For output characteristics, the channel current (I_{ds}) was measured as a function of drain voltage (V_{ds}) under a series of sweeping gate voltage (V_g). For transfer characteristics, V_{ds} was fixed at 2 V, while the channel current I_{ds} was measured as a function of gate voltage. Additionally, the response of FECTs is usually expressed as the ratio $(I_{on} - I_{off})/I_{off}$,[33] where I_{on} in this work represents the on current when the gate voltage is 0.5 V, which is also the working voltage during the subsequent experiments of dopamine sensing, and I_{off} refers to the off current when the gate voltage is 3.2 V. A set of cyclic curves were measured under a constant drain−source voltage, setting at 2 V. Furthermore, for the characterization of time-dependent I_{ds} about the FECT-based dopamine sensor, different concentrations of dopamine and interfering substances were added to the device under a fixed V_g = 0.5 V. For the investigation of superior sensitive DA sensors, the Pt and Au gate electrodes of the FECTs were modified with Nafion and were all prepared using the same method of PPy and nanofiber electrode.

3. RESULTS AND DISCUSSION

3.1. Morphology Characterizations. Figure 1a shows the morphology of preprocessed PA6 (85 D) filaments using

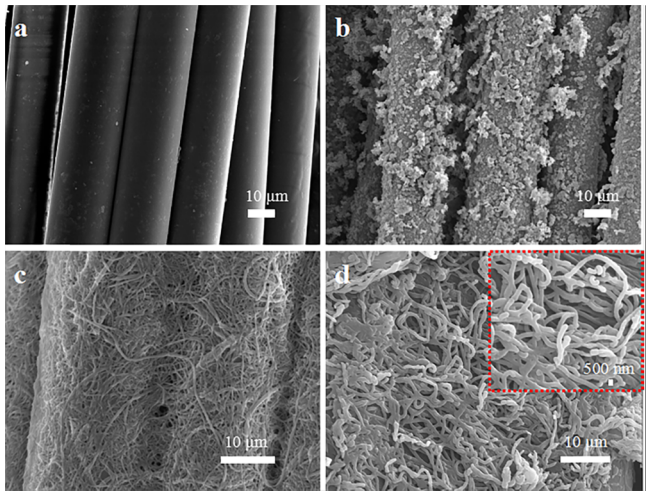

Figure 1. SEM images of (a) PA6, (b) PPy/PA6, (c) NFs/PA6, and (d) PPy/NFs/PA6.

scanning electron microscopy (SEM). The surfaces of PA6 filaments are smooth, and their diameters are in the range of 19−21 μm. For the PPy/PA6 filament (Figure 1b), PPy existed in the form of irregular granules and unevenly covered the surfaces of PA6 filaments. It can be obviously found that the PPy granules agglomerated and stacked together on PA6 filament surfaces. In Figure 1c, the NFs with diameters ranging from 100 to 500 nm entangled tightly with each other and adhered on the filament surface, forming a compact layer. This unique composite structure of NFs and the PA6 filament considerably increased their specific surface areas. In Figure 1d, the SEM image of PPy/NFs/PA6 showed that the introduction of NFs onto smooth PA6 filaments induced the morphology change of PPy from irregular granules into nanofibers with diameters in the range of 400−800 nm. The nanofibrous PPy interconnected together and formed three-dimensional (3D) network structures on the surface of the NFs/PA6 filament. IR spectroscopy (Figure S2) also confirmed the formation of PPy on PA6 filament surfaces. Compared to the PPy/PA6 filament, NFs undoubtedly play important roles in the appearance of these 3D interconnected PPy network structures. The existence of a large number of hydroxyl groups on PVA-*co*-PE nanofibers could significantly enhance the hydrophilicity of the PA6 filaments, improving the redox reaction active sites on surfaces to facilitate the in situ polymerization of Py. In addition, the PVA-*co*-PE nanofibers network was aligned randomly but intertwined tightly with each other on the PA6 filament surface, and the vast majority of gaps between each nanofiber were actually much smaller than the diameter of the PPy granule. As a result, the NFs could effectively provide a continuous growth template with an enormous surface area, making it possible for the formation of the PPy nanofiber network and significantly increasing the conductivity (Figure S3). The PPy nanofiber network-based electrode could improve ion adsorption, charge transfer, and carrier transport when it was assembled into a device.

3.2. Electrical Properties and Work Principle of FECTs. Electrical performance is one of the most momentous

DOI: 10.1021/acsami.9b00115
ACS Appl. Mater. Interfaces 2019, 11, 13105−13113

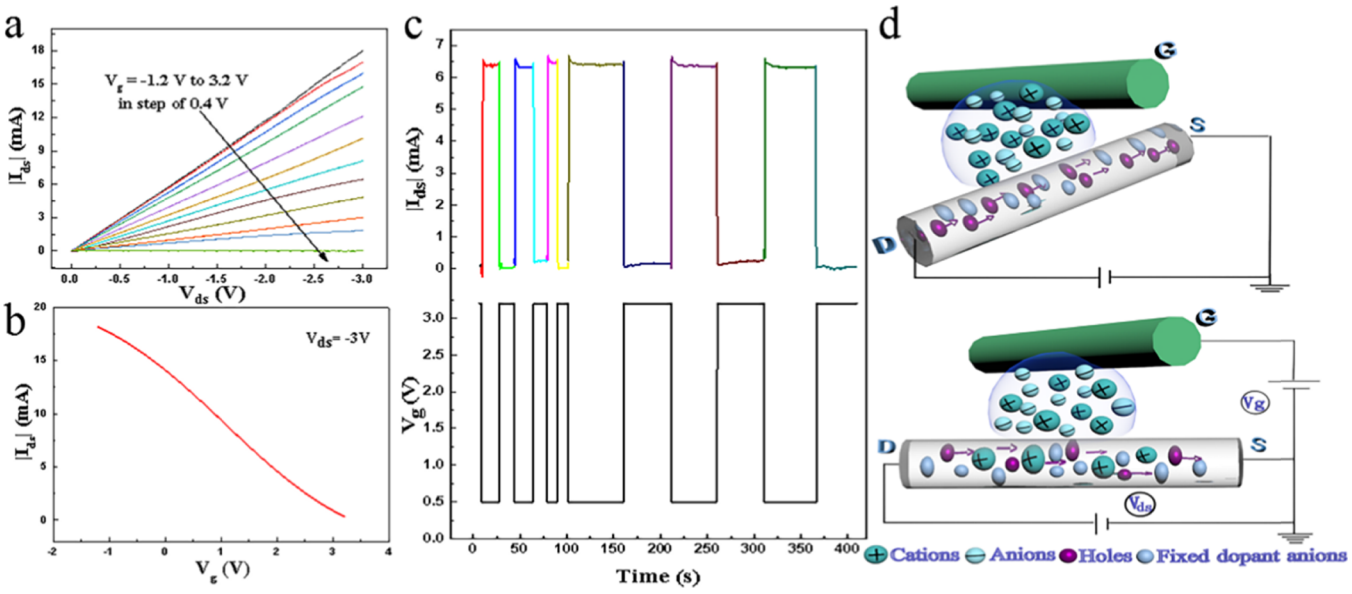

Figure 2. Electrical characteristics of FECTs. (a) Output curve of PPy/NFs/PA6-based FECTs. (b) Transfer curve of PPy/NFs/PA6-based FECTs. (c) Temporal response of the drain−source current (top panel) and gate voltage (bottom panel). (d) Logic circuit diagram and working principle of FECTs when no gate voltage (up) and positive gate voltage (down) are applied; the letters S, D, and G represent the source, drain, and gate electrode, respectively.

properties of conductive polymer materials. The appropriate working voltage and outstanding on/off ratio, together with fast and steady response time, exert a pivotal role in the application of FECTs. As shown in Figure 2a, the drain current presented a linear behavior at low applied voltages and a gradual saturation curve in the high voltage regime. Generally, the output characteristic curve of FECTs with the PPy nanofiber network as the active layer was in line with the law of a typical p-type depletion.[34] When the negative gate voltage was applied, the channel current I_{ds} increased. Upon sweeping increased positive voltages on the gate electrode, the channel current I_{ds} declined inversely. Figure 2b exhibits the transfer characteristic of the FECTs. For $V_g > 0$, the curve showed the transistor work in depletion mode. When $V_{ds} = -3$ V and $V_g =$ 0 V, a nonzero drain current was observed. When the positive gate voltage was applied, the channel was electrochemically reduced, resulting in the increase in electrical resistance and causing the decrease in I_{ds}. Figure 2c shows that it can gradually switch the FECTs from the on state to the off state. In this study, the on current is defined as the device's working current. Considering the subsequent working voltage in dopamine sensing, we denominated that the device was in its on state when V_g was 0.5 V and was switched off when V_g was changed to 3.2 V; the corresponding absolute on-current value was approximately 6.4 mA, and the average absolute off-current value was 2.5×10^{-2} mA, where the calculated ratio was 2.6×10^{2}. It could be deduced that the I_{on}/I_{off} ratio is up to two orders of magnitude, which is enough for the operation of devices.[35] Furthermore, for FECTs, the response time and stability during a period of time are decisive factors for its further application in biosensing. As shown in Figure 2c, the temporal response time and changes of I_{ds} between the on and off states were revealed. First, the temporal response of the device was extremely quick with a lower limit of 0.34 s from the off state to the on state (Figure S4), and the response time was fast in the fiber-based OECT field. According to the latest published results on the OECT-based DA sensor by Wang et al., the response time can shorten from 0.32 s to 5.58×10^{-5} s, which provides a new route for the further device performance study of FECTs.[19] The rapid response time benefited considerably from the nanostructure of the PPy/NFs/PA6 filament, which could accelerate the electron transfer and cation exchange rate between the electrolyte and channel. Second, the on/off current for each cycle was kept almost unchanged in the constant voltage. It was noteworthy that no sharp fluctuation was observed during these on/off cycles, which exhibited that the device could maintain continuous stability in repeated cycles. To deeply investigate the changes during the process, detailed electron and cation motion processes are presented in Figure 2d. The mechanism is elucidated as follows. During this process, a higher gate bias will contribute more cations from the electrolyte to inject into the PPy/NFs/PA6 backbone and aggravate the de-doping progress of the PPy, which accordingly leads to the reduction of the hole density and channel conductivity.[36]

3.3. Working Principle of FECT-Based Dopamine Sensor. To sufficiently take advantage of the FECTs, our research extends the knowledge into the application in dopamine sensing. For the FECT-based dopamine sensor, when the analysis substance dopamine (DA) was exposed to the device, it would be oxidized at the gate electrode immediately according to the following chemical reaction. In addition, *o*-dopamine quinone was the only end product, and two electrons were generated in this process; all of these directly resulted in a faradic current at the gate electrode and successfully converted the biochemical signal into an electronic one and a changed channel current.

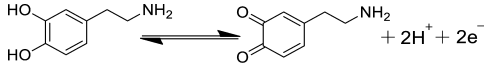

(1)

The channel current I_{ds} of the FECTs is determined by the factors given in eq 2[23,37]

DOI: 10.1021/acsami.9b00115
ACS Appl. Mater. Interfaces 2019, 11, 13105−13113

$$I_{ds} = \frac{q\mu p_0 tW}{LV_p}\left(V_p - V_g^{eff} + \frac{V_{ds}}{2}\right)V_{ds}, \text{ where } |V_{ds}| \ll |V_p - V_g^{eff}|, V_p = qp_0 t/c_i, \text{ and } V_g^{eff} = V_g + V_{offset} \quad (2)$$

where W and L represent the channel width and length of the FECT device, respectively. t is the thickness of the active layer, $q = 1.602 \times 10^{-19}$ is the electron charge, μ corresponds to the hole mobility of the organic semiconductor, and p_0 is the initial hole density in the PPy channel when $V_g = 0$ V. V_p is the pinch-off voltage of the transistor, while V_g^{eff} is the effective gate voltage. c_i is the effective gate capacitance per unit area of the FECT device. V_{offset} is an offset voltage determined by the potential drop between the gate/electrolyte interface and electrolyte/channel interface.[38]

Actually, the gate bias applied on the FECT device ultimately has complicated influences on the electrical potential of two interfaces, electrolyte/gate and electrolyte/channel interfaces. The gate voltage V_g can be defined by[37,39]

$$V_g = V_{g-e} + V_{e-c} = \left(1 + \frac{C_{e-c}}{C_{g-e}}\right)V_{e-c} = (1 + \gamma)V_{e-c} \quad (3)$$

where $V_{g\text{-}e}$ refers to the voltage applied on the electrolyte and gate interface, and $V_{e\text{-}c}$ is the voltage applied on the electrolyte and channel interface. In the same way, $C_{g\text{-}e}$ and $C_{e\text{-}c}$ are the capacitances of electrolyte/gate and electrolyte/channel interfaces, respectively, and the parameter $\gamma = \frac{C_{e-c}}{C_{g-e}}$. It was demonstrated that the electro-oxidation reaction of dopamine on the gate electrode was the direct reason for the decrease in $V_{g\text{-}e}$, which, in turn, resulted in the change in $V_{e\text{-}c}$ simultaneously and would also be affected due to the oxidation process. Both $V_{g\text{-}e}$ and $V_{e\text{-}c}$ can be derived from the Nernst equation in eq 4 as follows[26]

$$E_{Nernst} = E^{0'} + \frac{kT}{nq}\ln\left(\frac{[Ox]}{[Red]}\right) \quad (4)$$

where $E^{0'}$ is the formal potential, k is the Boltzmann constant, T is the Kelvin temperature, and n corresponds to the number of electrons transferred during the redox reaction; [Ox] and [Red] are the molar concentrations of oxidized and reduced species, respectively. In this system, DA is the oxidized material; when it was oxidized at the gate electrode, the generated electrons would gather at the electrolyte/gate interface. In turn, it impelled the cations from the electrolyte to flow toward the electrolyte/channel interface. The charge carrier distribution and potential drops between the gate and channel of the FECT in the presence of the analytical substance are shown in Figure 3.

In this process, $V_{g\text{-}e}$ and $V_{e\text{-}c}$ are altered and can be defined as eqs 5 and 6.[23] Moreover, it must be pointed out that $V_{e\text{-}c}$ can modulate the channel current straightway. By combining eqs 3 and 6, the relationship between the DA concentration and effective gate voltage (V_{gg}^{eff}) can be calculated as eq 7.[40]

$$V_{g-e} = -2.3\frac{kT}{2q}\log[C_{DA}] + A \quad (5)$$

$$V_{e-c} = V_g - V_{g-e} = V_g + 2.3\frac{kT}{2q}\log[C_{DA}] - A \quad (6)$$

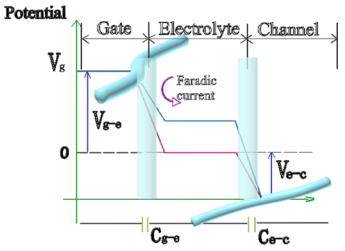

Figure 3. Potential diagram of the FECTs. (a) In the absence of dopamine (red line), the electrolyte potential is determined by the relative capacitances at the gate and channel interfaces. (b) In the presence of dopamine (blue line), the electrolyte potential is increased according to the Nernst equation.

$$V_g^{eff} = (1 + \gamma)V_{e-c} = 2.3(1 + \gamma)\frac{kT}{2q}\log[C_{DA}] + A^* \quad (7)$$

In these three equations, A and A^* represent two different constants. On the basis of the above equations, we conclude that the increasing DA concentration attribute to the decrease in $V_{g\text{-}e}$ and increase in both $V_{e\text{-}c}$ and V_g^{eff} Consequently, in terms of eqs 2 and 7, it is clear that the channel current is anticipated to decrease with the increase in V_g^{eff}

Similarly, the sensing mechanism of the FECT referring to AA, UA, and glucose are ascribed to the electro-oxidation of the interferents on the gate electrode, while every effective gate voltage is able to be calculated in the same way; the results are obtained as follows[38]

$$V_g^{eff} = 2.3(1 + \gamma)\frac{kT}{2q}\log[C_{AA}] + B \quad (8)$$

$$V_g^{eff} = 2.3(1 + \gamma)\frac{kT}{2q}\log[C_{UA}] + C \quad (9)$$

$$V_g^{eff} = 2.3(1 + \gamma)\frac{kT}{2q}\log[C_{glucose}] + D \quad (10)$$

where B, C, and D are three different constants.

3.4. Performance of Dopamine Sensing. In the past decades, tremendous efforts have been devoted to the Pt electrode-based OECTs.[17,41] In this study, a low-cost and high-throughput-fabrication FECT device has been successfully designed, which may provide an efficient and powerful platform for the sensing of dopamine and open the door to new possibilities in portable and wearable electrical sensing equipment.

Figure 4a compares the responses of absolute channel current for three types of FECTs when six groups of consecutive DA concentrations were added to the sensors under the same condition. The involved test procedure is illustrated in the Supporting Information. The difference between these three FECTs lies in the material of the gate electrode. First of all, it was important to highlight that the PPy/NFs/PA6 (85 D)-based FECT had the biggest initial absolute channel current compared to the Pt-based FECTs. Nevertheless, the absolute current of a Au-based FECT was consistently lower than the other two during the whole test period. The distinct difference in initial current illustrated that the excellent electrical property of the conductive polymer materials, PPy/NFs/PA6 (85 D), was comparable with metal and even more suitable for the application of the FECT-based dopamine sensor since the larger initial current was more

DOI: 10.1021/acsami.9b00115
ACS Appl. Mater. Interfaces 2019, 11, 13105−13113

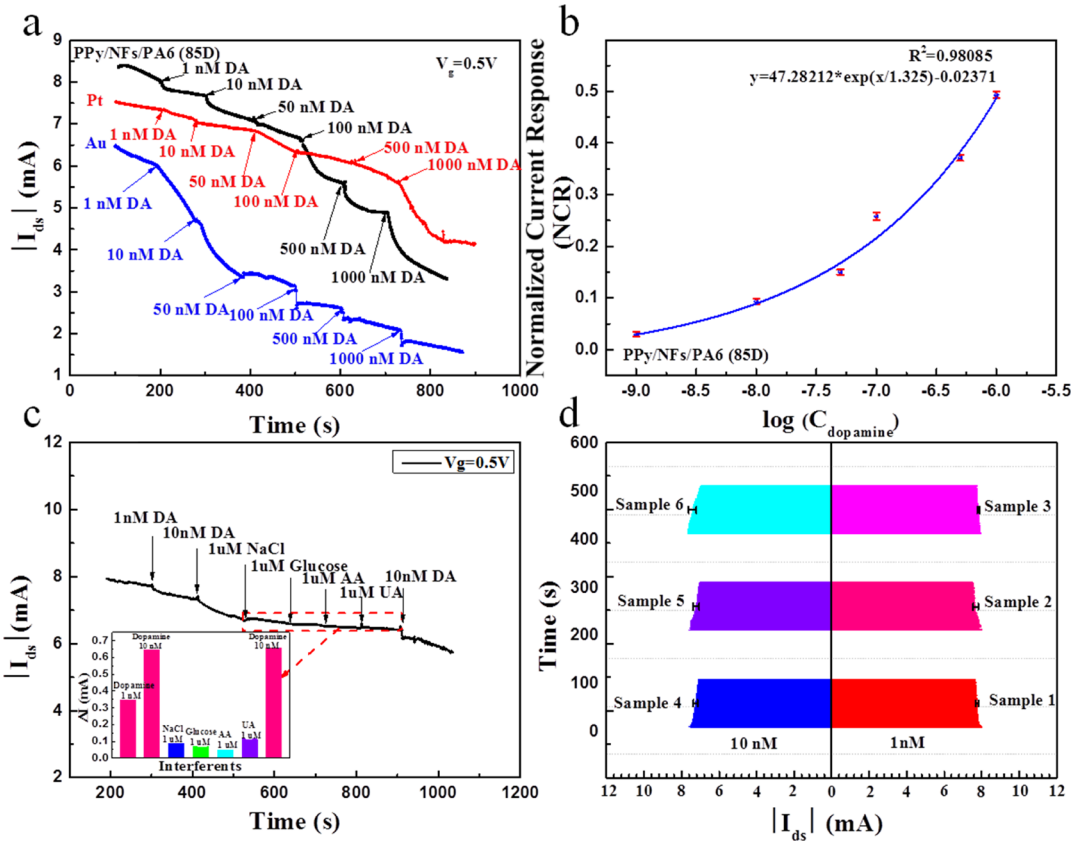

Figure 4. (a) Response of the FECTs with PPy/NFs/PA6, Pt, and Au gate electrodes to additions of dopamine in PBS solution from the concentrations of dopamine between 1 and 1000 nM. (b) Normalized current response versus log($C_{dopamine}$). The curve line is the exponent fit to the data of dopamine concentration. (c) Amperometric responses of the FECT sensor upon additions of 1 nM dopamine, 10 nM dopamine, 1 μM NaCl, 1 μM glucose, 1 μM AA, 1 μM UA, and 10 nM dopamine in PBS when V_g = 0.5 V. Inset: bar diagram of normalized amperometric current versus interferents. (d) Repeatability test of the biosensors based on FECTs.

observable. Furthermore, because of the significant cost differences, the PPy/NFs/PA6 filament was identified as an ideal material for the FECT-based DA sensor. Subsequently, starting from 200 s, a set of dopamine drops with stepwisely increased concentrations (from 1 to 1000 nM) were added to the three FECT systems every 100 s. It was particularly noticeable that all the channel currents showed a downward trend when dopamine was contacted and oxidized at gate electrodes. In addition, the sensor current would change immediately within 0.5 s every time when the DA analyte was added to the sensor; this rapid response time was much shorter than the reports in another paper.[42] Although the overall current decrease in amplitude for the PPy/NFs/PA6 (85 D)-based FECT was similar to the Pt-based FECT, the variation amplitudes of the channel current for the former one increased gradually with ascending DA concentrations. Compared to the other two electrodes, it existed obviously different from the concentrations of 100 to 1000 nM. The excellent electrical conductivity, DA sensibility, and the fast response time were likely due to the PPy nanofiber network on the filament; the enormous specific surface area ensured the DA to be oxidized adequately on the gate electrode compared to smooth metal electrodes. Furthermore, the weak DA concentration signal input in the FECTs could yield a considerable large response in the current outputs.

Usually, to compare the current response to different FECTs, the normalized current response $(I - I_0)/I_0$ was investigated as a function of the DA concentration in the range of 1−1000 nM, where I_0 was the current when dopamine was not added, and I was the current when dopamine was exposed to the gate electrode of the PPy/NFs/PA6 (85 D)-based FECTs. Figure 4b indicates that the FECT exhibited a good exponential function relationship between the logarithm of dopamine concentration and normalized current response (NCR). According to the exponent fitted curve, a sensitivity of 47.28 NCR per decade was obtained, and the correlation coefficient (R^2) was 0.98085. Different from the common linear current response reported in another literature,[43] the result implicates a new rule for the NCR curve. In addition, it is significant that the current variation amplitude becomes more and more obvious if the DA-detecting concentrations increased, which, in turn, proves that the FECT-based sensor is a promising candidate for dopamine sensing.

Furthermore, to investigate the specificity, the responses of the FECT-based dopamine sensor to several interfering substances are imperative. As shown in Figure 4c, NaCl, UA, AA, and glucose were chosen as the interferents because they were dominant in body fluids and the concentrations of AA and UA were usually several orders of magnitude higher than that of DA.[25] Hence, herein, their concentrations were all set at 1 μM, ensuring that they are considerably larger than the detecting concentration of dopamine. When the interferents were added to the FECT-based sensor in sequence, the reduction of the absolute current for each was 1.7% (NaCl), 1.2% (glucose), 1.3% (AA), and 1.4% (UA). Nevertheless, the corresponding values to 1 and 10 nM dopamine in this

DOI: 10.1021/acsami.9b00115
ACS Appl. Mater. Interfaces 2019, 11, 13105−13113

experiment were 3.7%, 8.1% (the first time), and 8.3% (the second time). The inset of Figure 4c shows the relationship between the current responses and analytes, indicating that the PPy/NFs/PA6 (85 D)-based FECTs were highly specific to dopamine even in the presence of relatively high concentrations of interferents.

It is generally accepted that reproducibility plays a critical role in the sensing applications, especially when the concentration of dopamine is extremely low. To further confirm the property of FECT-based dopamine sensors, many efforts had been made to examine its reproducibility. As shown in Figure 4d, when detecting 1 nM dopamine, all the samples (from samples 1 to 3) exhibited similar current responses during 100 s, and the values of the corresponding absolute currents were consistent with those obtained in Figure 4a. Meanwhile, under the same condition, identical results were also found when using another group of samples (from samples 4 to 6) to detect 10 nM dopamine. On the basis of these results, the device shows excellent reproducibility.

3.5. Wearable Devices. To verify the possibility of woven FECTs and their circuit array, some devices were devised as follows. All of the woven fabrics were obtained by an ordinary loom shown in Figure 5a. As shown in Figure 5b, an independent fabric product with an integrated FECT circuit was woven with a length of more than 28 cm. Inspired by the physical structure of the woven products, the PPy/NFs/PA6 electrodes were first seamed into a special woven product without an FECT unit, as shown in Figure 5c. The devices prepared were flexible and could maintain a good crisscross shape. After all of the attempts mentioned above, the PPy/NFs/PA6 electrodes were directly woven into the products during weaving. As shown in Figure 5d, the FECT unit could be tightly immobilized in the product even when fitted to the human wrist and forehead skin.

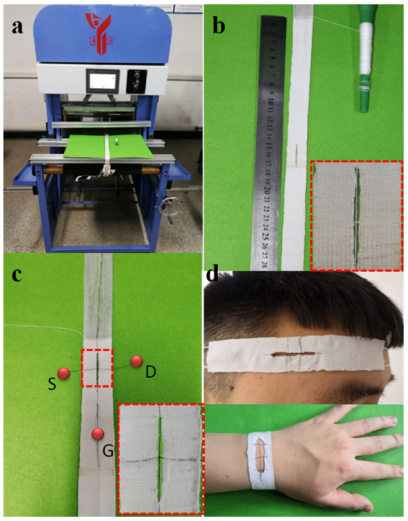

Figure 5. Image of woven fiber-based organic electrochemical transistors (FECTs). (a) Image of the loom. (b) Woven fabric with a single FECT circuit. (c) Woven single FECT circuit with PPy/NFs/PA6 fiber. (d) Woven series arrayed FECT circuit with PPy/NFs/PA6 fiber in the wearable point-of-care applications.

Furthermore, despite the good device performances referred in the paper, the future of the practical performance of the FECT-based device looks bright when taking the aesthetics into consideration by changing the woven stitch structure.

3.6. Real Sample Analysis. To evaluate the practical performance for the analysis of a real sample, the FECT-based sensor was applied for the determination of DA in human injection samples. The injection samples from the hospital were diluted with phosphate buffer solution for the detection of dopamine. Different concentrations of DA were prepared by diluting the solution of the real samples. The results obtained using the prepared FECTs were compared with known dopamine concentrations. The result of every set of DA concentration was calculated from the average value of three groups of tests. The FECT response results to 10, 50, 100, 500, and 1000 nM diluted human injection DA solutions are shown in Table 1. It should be noted that the root-mean-square error (RMSE) was small at a very low DA concentration, indicating that the proposed dopamine sensor was applicable for the practical applications.

Table 1. Determination of Dopamine Injection Samples Using FECT-Based Dopamine Sensors

C_{DA}	log[C]	average log[C] determined by FECTs	average root-mean-square error (RMSE)
10 nM	−8.00	−8.01	0.08
50 nM	−7.30	−7.45	0.05
100 nM	−7.00	−6.81	0.12
500 nM	−6.30	−6.40	0.09
1000 nM	−6.00	−6.02	0.15

4. CONCLUSIONS

In this study, a novel PPy/NFs/PA6 filament-based electrochemical transistor was designed and fabricated. The sole modification method was implemented by compounding a layer of PVA-*co*-PE nanofibers on the PA6 filament. Interestingly, the introduction of the PVA-*co*-PE nanofiber onto the PA6 filament surfaces significantly changed the morphology of in situ-polymerized Py from irregular granules to interconnected nanofibers, facilitating the formation of the PPy nanofiber network layer on PA6 filaments. The unique surface structures of PVA-*co*-PE and PPy NFs improved the specific surface area of the PA6 filament and the conductivity of the PPy/NFs/PA6 filament. The FECTs prepared with the PPy/NFs/PA6 filament exhibited outstanding electrical performances, such as large on/off ratio up to 10^2, short response time of 0.34 s, and good cycle stability. Subsequently, compared with FECTs with metal as gate electrodes, the sensing behaviors of FECTs with a PPy/NFs/PA6 electrode demonstrated the larger initial channel current, better sensibility to DA, shorter response time within 0.5 s, higher sensitivity of 47.28 NCR per decade, ultraspecificity in the presence of NaCl, glucose, AA, and UA, and outstanding repeatability. The results suggest that the PPy/NFs/PA6-based organic electrochemical transistors may provide a viable source for high sensitivity, selectivity, and economical wearable DA sensors.

■ ASSOCIATED CONTENT

Supporting Information

The Supporting Information is available free of charge on the ACS Publications website at DOI: 10.1021/acsami.9b00115.

Device structure, FT-IR spectroscopy, conductivity, response time, and the dopamine test process; the woven looming draft of FECTs, woven fabric samples,

DOI: 10.1021/acsami.9b00115
ACS Appl. Mater. Interfaces 2019, 11, 13105−13113

device response to a certain DA concentration, and bending stability of PVA/NFs/PA6 filaments (PDF)

AUTHOR INFORMATION

Corresponding Authors

*E-mail: wydan2015@163.com (Y.W.).
*E-mail: wangdon08@126.com (D.W.).

ORCID

Dong Wang: 0000-0002-8139-8502
Qiongzhen Liu: 0000-0003-3087-6081
Ke Liu: 0000-0002-5090-8186

Notes

The authors declare no competing financial interest.

ACKNOWLEDGMENTS

This study was financially supported by the National Natural Science Foundation of China (grant nos. 51503157, 51873166, and 51603155), the Program for Provincial and Ministerial Base Platform of Hubei (2017AHB065), and the Science and Technology Program of Wuhan Technology Bureau (2017060201010165). The authors also acknowledge for the financial support from Wuhan Advanced Fiber Engineering Technology Research Center and the Hubei Province Central Government Guides Local Science and Technology Development Projects (2018ZYYD057).

REFERENCES

(1) Phillips, P. E. M.; Stuber, G. D.; Heien, M. L. A. V.; Wightman, R. M.; Carelli, R. M. Subsecond Dopamine Release Promotes Cocaine Seeking. *Nature* **2003**, *422*, 614−618.

(2) Yang, W.; Yu, Y.; Tang, Y.; Li, K.; Zhao, Z.; Li, M.; Yin, G.; Li, H.; Sun, S. Enhancing Electrochemical Detection of Dopamine via Dumbbell-like FePt−Fe_3O_4 Nanoparticles. *Nanoscale* **2017**, *9*, 1022−1027.

(3) Tang, H.; Lin, P.; Chan, H. L. W.; Yan, F. Highly Sensitive Dopamine Biosensors Based on Organic Electrochemical Transistors. *Biosens. Bioelectron.* **2011**, *26*, 4559−4563.

(4) Li, B. R.; Hsieh, Y. J.; Chen, Y. X.; Chung, Y. T.; Pan, C. Y.; Chen, Y. T. An Ultrasensitive Nanowire-transistor Biosensor for Detecting Dopamine Release from Living PC12 Cells under Hypoxic Stimulation. *J. Am. Chem. Soc.* **2013**, *135*, 16034−16037.

(5) Nagal, A.; Singla, R. K. Parkinson's Disease: Diagnosis, Therapeutics & Management. *WebmedCentral Pharm. Sci.* **2012**, *3*, WMC003670.

(6) Wortmann, M. Dementia: A Global Health Priority-highlights from an ADI and World Health Organization report. *Alzheimer's Res. Ther.* **2012**, *4*, 40−43.

(7) Wang, W.; Xu, G.; Cui, X. T.; Sheng, G.; Luo, X. Enhanced Catalytic and Dopamine Sensing Properties of Electrochemically Reduced Conducting Polymer Nanocomposite Doped with Pure Graphene Oxide. *Biosens. Bioelectron.* **2014**, *58*, 153−156.

(8) Feng, X.; Zhang, Y.; Zhou, J.; Li, Y.; Chen, S.; Zhang, L.; Ma, Y.; Wang, L.; Yan, X. Three-dimensional Nitrogen-doped Graphene as an Ultrasensitive Electrochemical Sensor for The Detection of Dopamine. *Nanoscale* **2015**, *7*, 2427−2432.

(9) Fu, X.; Tan, X.; Yuan, R.; Chen, S. A Dual-potential Electrochemiluminescence Ratiometric Sensor for Sensitive Detection of Dopamine Based on Graphene-CdTe Quantum Dots and Self-enhanced Ru (II) Complex. *Biosens. Bioelectron.* **2017**, *90*, 61−68.

(10) Li, X.; Pan, J.; Yang, F.; Feng, J.; Mo, J.; Chen, Z. Simple Amperometric Detector for Microchip Capillary Electrophoresis, And Its Application To The Analysis of Dopamine and Catechol. *Microchim. Acta* **2011**, *174*, 123−130.

(11) Clarke, S. J.; Hollmann, C. A.; Zhang, Z.; Suffern, D.; Bradforth, S. E.; Dimitrijevic, N. M.; Minarik, W. G.; Nadeau, J. L. Photophysics of Dopamine-modified Quantum Dots and Effects on Biological Systems. *Nat. Mater.* **2006**, *5*, 409−417.

(12) Hubbard, K. E.; Wells, A.; Owens, T. S.; Tagen, M.; Fraga, C. H.; Stewart, C. F. Determination of Dopamine, Serotonin, and Their Metabolites in Pediatric Cerebrospinal Fluid by Isocratic High Performance Liquid Chromatography Coupled with Electrochemical Detection. *Biomed. Chromatogr.* **2010**, *24*, 626−631.

(13) Wang, Y.; Li, Y.; Tang, L.; Lu, J.; Li, J. Application of Graphene-modified Electrode for Selective Detection of Dopamine. *Electrochem. Commun.* **2009**, *11*, 889−892.

(14) Zhao, H.; Zhang, Y.; Yuan, Z. Study on The Electrochemical Behavior of Dopamine with Poly (sulfosalicylic acid) Modified Glassy Carbon Electrode. *Anal. Chim. Acta* **2001**, *441*, 117−122.

(15) Liao, C.; Zhang, M.; Niu, L.; Zheng, Z.; Yan, F. Organic Electrochemical Transistors with Graphene-modified Gate Electrodes for Highly Sensitive and Selective Dopamine Sensors. *J. Mater. Chem. B* **2014**, *2*, 191−200.

(16) Wang, N.; Yang, A.; Fu, Y.; Li, Y.; Yan, F. Functionalized Organic Thin Film Transistors for Biosensing. *Acc. Chem. Res.* **2019**, *52*, 277−287.

(17) Tang, H.; Yan, F.; Lin, P.; Xu, J.; Chan, H. L. W. Highly Sensitive Glucose Biosensors Based on Organic Electrochemical Transistors Using Platinum Gate Electrodes Modified with Enzyme and Nanomaterials. *Adv. Funct. Mater.* **2011**, *21*, 2264−2272.

(18) Fu, Y.; Wang, N.; Yang, A.; Law, H. K.-w.; Li, L.; Yan, F. Highly Sensitive Detection of Protein Biomarkers with Organic Electrochemical Transistors. *Adv. Mater.* **2017**, *29*, 1703787.

(19) Wang, N.; Liu, Y.; Fu, Y.; Yan, F. AC Measurements Using Organic Electrochemical Transistors for Accurate Sensing. *ACS Appl. Mater. Interfaces* **2018**, *10*, 25834−25840.

(20) Braendlein, M.; Pappa, A.-M.; Ferro, M.; Lopresti, A.; Acquaviva, C.; Mamessier, E.; Malliaras, G. G.; Owens, R. M. Lactate Detection In Tumor Cell Cultures Using Organic Transistor Circuits. *Adv. Mater.* **2017**, *29*, 1605744.

(21) Lin, P.; Yan, F.; Chan, H. L. W. Ion-sensitive Properties of Organic Electrochemical Transistors. *ACS Appl. Mater. Interfaces* **2010**, *2*, 1637−1641.

(22) Sessolo, M.; Rivnay, J.; Bandiello, E.; Malliaras, G. G.; Bolink, H. J. Ion-Selective Organic Electrochemical Transistors. *Adv. Mater.* **2014**, *26*, 4803−4807.

(23) Liao, C.; Mak, C.; Zhang, M.; Chan, H. L. W.; Yan, F. Flexible Organic Electrochemical Transistors for Highly Selective Enzyme Biosensors and Used for Saliva Testing. *Adv. Mater.* **2015**, *27*, 676−681.

(24) Lin, P.; Luo, X.; Hsing, I.-M.; Yan, F. Organic Electrochemical Transistors Integrated in Flexible Microfluidic Systems and Used for Label-free DNA Sensing. *Adv. Mater.* **2011**, *23*, 4035−4040.

(25) Gualandi, I.; Tonelli, D.; Mariani, F.; Scavetta, E.; Marzocchi, M.; Fraboni, B. Selective Detection of Dopamine with An All PEDOT: PSS Organic Electrochemical Transistor. *Sci. Rep.* **2016**, *6*, 35419.

(26) Wang, Y.; Qing, X.; Zhou, Q.; Zhang, Y.; Liu, Q.; Liu, K.; Wang, W.; Li, M.; Lu, Z.; Chen, Y.; Wang, D. The Woven Fiber Organic Electrochemical Transistors Based on Polypyrrole Nanowires/reduced Graphene Oxide Composites for Glucose Sensing. *Biosens. Bioelectron.* **2017**, *95*, 138−145.

(27) Yang, A.; Li, Y.; Yang, C.; Fu, Y.; Wang, N.; Li, L.; Yan, F. Fabric Organic Electrochemical Transistors for Biosensors. *Adv. Mater.* **2018**, *30*, 1800051.

(28) Xiong, B.; Zhong, W.; Zhu, Q.; Liu, K.; Li, M.; Sun, G.; Wang, D. Highly Transparent and Rollable PVA-co-PE Nanofibers Synergistically Reinforced With Epoxy Film for Flexible Electronic Devices. *Nanoscale* **2017**, *9*, 19216−19226.

(29) Wang, D.; Sun, G.; Chiou, B.-S. A High-throughput, Controllable, and Environmentally Benign Fabrication Process of Thermoplastic Nanofibers. *Macromol. Mater. Eng.* **2007**, *292*, 407−414.

(30) Tao, Y.; Liu, Q.; Chen, J.; Wang, B.; Wang, Y.; Liu, K.; Li, M.; Jiang, H.; Lu, Z.; Wang, D. Hierarchically Three-dimensional

DOI: 10.1021/acsami.9b00115
ACS Appl. Mater. Interfaces 2019, 11, 13105−13113

Nanofiber Based Textile with High Conductivity and Biocompatibility as A Microbial Fuel Cell Anode. *Environ. Sci. Technol.* **2016**, *50*, 7889−7895.
(31) Li, M.; Li, H.; Zhong, W.; Zhao, Q.; Wang, D. Stretchable Conductive Polypyrrole/polyurethane (PPy/PU) Strain Sensor with Netlike Microcracks for Human Breath Detection. *ACS Appl. Mater. Interfaces* **2014**, *6*, 1313−1319.
(32) Wang, Y.; Zhang, Y.; Zhong, W.; Qing, X.; Zhou, Q.; Liu, Q.; Wang, W.; Liu, X.; Li, M.; Wang, D. Flexible Supercapacitor With High Energy Density Prepared by GO-induced Porous Coral-like Polypyrrole (PPy)/PET Non-woven Fabrics. *J. Mater. Sci.* **2018**, *53*, 8409−8419.
(33) Campana, A.; Cramer, T.; Simon, D. T.; Berggren, M.; Biscarini, F. Electrocardiographic Recording with Conformable Organic Electrochemical Transistor Fabricated on Resorbable Bioscaffold. *Adv. Mater.* **2014**, *26*, 3874−3878.
(34) Khodagholy, D.; Rivnay, J.; Sessolo, M.; Gurfinkel, M.; Leleux, P.; Jimison, L. H.; Stavrinidou, E.; Herve, T.; Sanaur, S.; Owens, R. M.; Malliaras, G. G. High Transconductance Organic Electrochemical Transistors. *Nat. Commun.* **2013**, *4*, 2133−2138.
(35) Müller, C.; Hamedi, M.; Karlsson, R.; Jansson, R.; Marcilla, R.; Hedhammar, M.; Inganäs, O. Woven Electrochemical Transistors on Silk Fibers. *Adv. Mater.* **2011**, *23*, 898−901.
(36) Bernards, D. A.; Malliaras, G. G. Steady-State and Transient Behavior of Organic Electrochemical Transistors. *Adv. Funct. Mater.* **2007**, *17*, 3538−3544.
(37) Liao, J.; Lin, S.; Zeng, M.; Yang, Y. A Miniature Photoelectrochemical Sensor Based on Organic Electrochemical Transistor for Sensitive Determination of Chemical Oxygen Demand in Wastewaters. *Water Res.* **2016**, *94*, 296−304.
(38) Zhang, L.; Wang, G.; Wu, D.; Xiong, C.; Zheng, L.; Ding, Y.; Lu, H.; Zhang, G.; Qiu, L. Highly Selective and Sensitive Sensor Based on An Organic Electrochemical Transistor for the Detection of Ascorbic Acid. *Biosens. Bioelectron.* **2018**, *100*, 235−241.
(39) Gualandi, I.; Scavetta, E.; Mariani, F.; Tonelli, D.; Tessarolo, M.; Fraboni, B. All Poly (3, 4-Ethylenedioxythiophene) Organic Electrochemical Transistor to Amplify Amperometric Signals. *Electrochim. Acta* **2018**, *268*, 476−483.
(40) Cicoira, F.; Sessolo, M.; Yaghmazadeh, O.; DeFranco, J. A.; Yang, S. Y.; Malliaras, G. G. Influence of Device Geometry on Sensor Characteristics of Planar Organic Electrochemical Transistors. *Adv. Mater.* **2010**, *22*, 1012−1016.
(41) Rivnay, J.; Inal, S.; Salleo, A.; Owens, R. M.; Berggren, M.; Malliaras, G. G. Organic Electrochemical Transistors. *Nat. Rev. Mater.* **2018**, *3*, 17086−17090.
(42) Macaya, D. J.; Nikolou, M.; Takamatsu, S.; Mabeck, J. T.; Owens, R. M.; Malliaras, G. G. Simple Glucose Sensors with Micromolar Sensitivity Based on Organic Electrochemical Transistors. *Sens. Actuators, B* **2007**, *123*, 374−378.
(43) Kergoat, L.; Piro, B.; Simon, D. T.; Pham, M. C.; Noël, V.; Berggren, M. Detection of Glutamate and Acetylcholine with Organic Electrochemical Transistors Based on Conducting Polymer/Platinum Nanoparticle Composites. *Adv. Mater.* **2014**, *26*, 5658−5664.

DOI: 10.1021/acsami.9b00115
ACS Appl. Mater. Interfaces 2019, 11, 13105−13113